

Self-Assembled Monolayers of Phosphonic Acids with Enhanced Surface Energy for High-Performance Solution-Processed N-Channel Organic Thin-Film Transistors**

Danqing Liu, Xiaomin Xu, Yaorong Su, Zikai He, Jianbin Xu, and Qian Miao*

A self-assembled monolayer (SAM) is only a few nanometers thick, but can dramatically change the surface properties.^[1] Herein we report novel SAMs of phosphonic acids (shown in Figure 1 a), which are completely wettable by various organic solvents because of the enhanced surface energy of the SAMs, leading to solution-processed n-channel organic thin-film transistors (OTFTs) with average field effect mobility as high as $1.6 \text{ cm}^2 \text{ V}^{-1} \text{ s}^{-1}$. OTFTs are elemental units in organic integrated circuits that, for example, operate radio-frequency identification (RFID) tags and sensors and are used to drive individual pixels in active matrix displays.^[2,3] For these applications, solution-processed OTFTs can be fabricated onto flexible substrates over a large area at low cost using roll-to-roll or ink-jet printing techniques. OTFTs are interface devices with their performance highly dependent on the interface between organic semiconductors and gate dielectrics no matter whether the organic semiconductors are processed by vacuum deposition or solution-based methods. Owing to the key importance of the semiconductor–dielectric interface, great efforts have been made in interface engineering to control the interface structures, such as molecular ordering, surface dipoles, and film morphology. By virtue of their ability to manipulating the surface properties, SAMs of organosilanes and phosphonic acids^[4] have been developed as a very powerful tool to modify the dielectric oxide surface in OTFTs, particularly vacuum-deposited OTFTs. It is worth noting that the success of a specific SAM in vacuum-deposited OTFTs is often barely duplicated in solution-processed OTFTs, and controlling the morphology of solution-processed films of organic semiconductors is usually complex.^[5] One key factor that affects the nucleation and

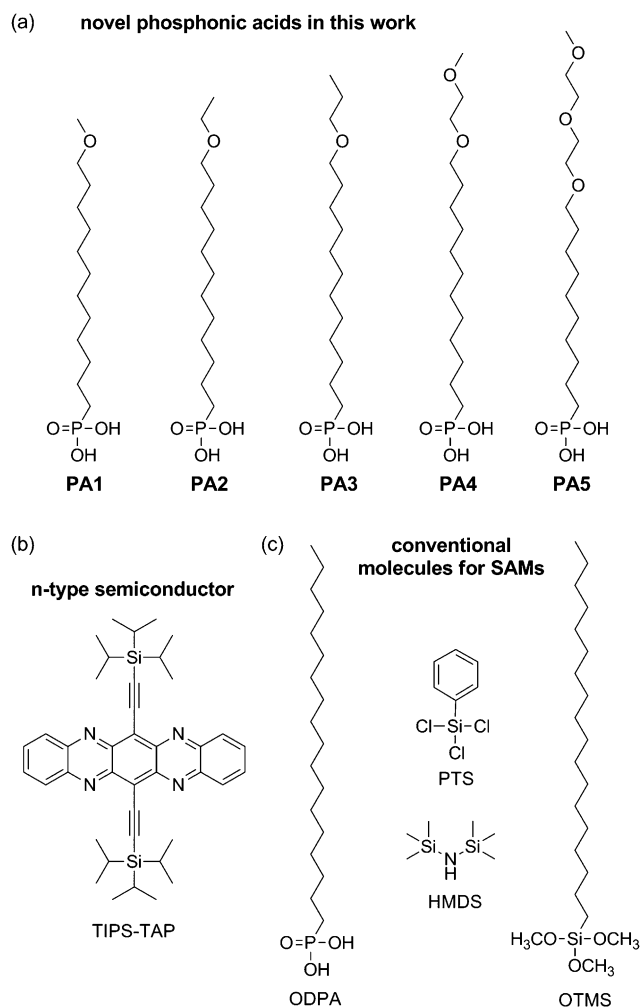


Figure 1. Structural formula of a) novel phosphonic acids that have polar oxygen atoms inserted into the long alkyl chain; b) n-type semiconductor TIPS-TAP; c) conventional molecules that form SAMs on the dielectric surface of OTFTs.

growth of semiconductor molecules during solution-based processing is the wetting behavior of the semiconductor solution on the dielectric surface.^[6] For example, the methyl terminated long-chain SAMs, such as octadecylphosphonic acid (ODPA)^[7] and octadecyltrimethoxysilane (OTMS)^[8] as shown in Figure 1c, are found very useful in vacuum-deposited OTFTs leading to high field effect mobility for holes and electrons, but exhibit low surface energy making solution processing of small-molecule organic semiconductors onto these dielectric surfaces challenging.^[5,9]

[*] D. Liu, X. Xu, Z. He, Prof. Q. Miao
Department of Chemistry, The Chinese University of Hong Kong
Shatin, New Territories, Hong Kong (China)
E-mail: miaoqian@cuhk.edu.hk

Y. Su, Prof. J. Xu
Department of Electronic Engineering
The Chinese University of Hong Kong
Shatin, New Territories, Hong Kong (China)

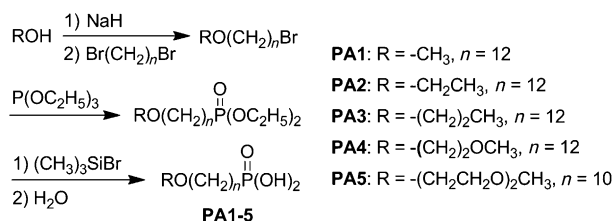
Prof. J. Xu, Prof. Q. Miao
Institute of Molecular Functional Materials (Areas of Excellence
Scheme, University Grants Committee), Hong Kong (China)

[**] This work was supported by grants from the Research Grants
Council (project number: CUHK2/CRF/08) and the University
Grants Committee, Hong Kong SAR, China (project number: AoE/
P-03/08).

Supporting information for this article is available on the WWW
under <http://dx.doi.org/10.1002/anie.201300353>.

The soluble n-type organic semiconductor used in this study is 6,13-bis((triisopropylsilyl)ethynyl)-5,7,12,14-tetraazapentacene (TIPS-TAP as shown in Figure 1b), which was synthesized by modifying the reported procedures^[10] as detailed in the Supporting Information. This modified synthesis led to TIPS-TAP in higher yield and purity. As reported by us earlier, TIPS-TAP exhibited an average electron mobility of $1.6 \text{ cm}^2 \text{ V}^{-1} \text{ s}^{-1}$ in vacuum-deposited thin-film transistors when the SiO_2 dielectric surface was modified with a SAM of OTMS.^[11] However, fabricating OTFTs by drop-casting solutions of TIPS-TAP onto the same OTMS-modified SiO_2 surface appeared problematic because of the poor wettability of such a dielectric surface. Most of common organic solvents led to thick crystals that were not suitable for fabricating OTFTs,^[12] while only hexane led to continuous films with low field effect mobility of up to $0.02 \text{ cm}^2 \text{ V}^{-1} \text{ s}^{-1}$ as detailed in the Supporting Information. On the other hand, solutions of TIPS-TAP in chlorobenzene did form continuous films on bare SiO_2 , but only showed a low field effect mobility of $3 \times 10^{-3} \text{ cm}^2 \text{ V}^{-1} \text{ s}^{-1}$,^[11] presumably because of the electron trapping by hydroxy groups on the SiO_2 surface.^[13] To solve this dilemma, a SAM with higher surface energy than OTMS is necessary. The SAMs of phenyltrichlorosilane (PTS as shown in Figure 1c) and hexamethyldisilazane (HMDS as shown in Figure 1c), which were reported to have higher surface energy and thus be wettable by several organic semiconductor solutions, were used to modify the SiO_2 dielectric surface. But they only led to drop-cast films of TIPS-TAP with low field effect mobility in the range of $10^{-3} \text{ cm}^2 \text{ V}^{-1} \text{ s}^{-1}$ presumably because of the morphology of the resulting films as detailed below. To develop new SAMs with enhanced surface energy suitable for solution-processed n-channel OTFTs, we designed novel phosphonic acids (**PA1–5**) that have polar oxygen atoms inserted into the long alkyl chain (Figure 1a). This design has phosphonic acid as the anchoring group because phosphonic acids are stable and easily purified, and has methyl as the terminal group to avoid electron trapping by hydroxy groups. To better understand the relationship between the molecular structures and the wettability of SAMs, the number and position of oxygen atoms are varied. By allowing these phosphonic acids to self-assemble on a solution-processed high- k metal oxide layer,^[14] we were able to fabricate wettable dielectrics for solution-processed n-channel OTFTs of TIPS-TAP with high field effect mobility and low operation voltage.

Phosphonic acids **PA1–5** were synthesized from the corresponding alcohols and dibromoalkanes in three steps as shown in Scheme 1. To facilitate the fabrication of OTFTs,



Scheme 1. Synthesis of phosphonic acids **PA1–5**.

a thin layer of $\text{AlO}_y/\text{TiO}_x$ was deposited on a highly doped silicon wafer following the reported spin-coating procedure to form dielectrics.^[14] $\text{AlO}_y/\text{TiO}_x$ rather than SiO_2 was used as the dielectric layer because long-chain phosphonic acids efficiently bind to metal oxides with stable P-O-M phosphonate bonds resulting in highly ordered and densely packed SAMs.^[15] Following the reported procedure for forming SAMs of phosphonic acids on AlO_x ,^[5,7] **PA1–5** were then allowed to self-assemble on the surface of $\text{AlO}_y/\text{TiO}_x$ by soaking the metal oxide coated Si wafer in a solution of the phosphonic acid in isopropanol at room temperature for 12 h. The resulting SAM-modified dielectric was characterized in terms of roughness, capacitance, leakage current, and surface energy. It is found that **PA1–5** generally form a very smooth surface with a root mean square (RMS) roughness of 0.2 nm over an area of $25 \mu\text{m}^2$ as measured by atomic force microscopy (AFM). Such roughness is comparable to that of the ultrasmooth SAMs of OTMS on SiO_2 .^[8] The capacitance per unit area (C_i) for the dielectric modified with different phosphonic SAMs was measured from a metal-insulator-metal structure using vacuum-deposited gold as the top electrode with the frequency ranging from 100 Hz to 100 kHz.^[16] Very similar to the bare $\text{AlO}_y/\text{TiO}_x$ dielectric,^[14] the SAM-modified $\text{AlO}_y/\text{TiO}_x$ dielectric exhibits a slightly decreased capacitance per unit area with increased frequency. Such frequency-dependent capacitance is often related to the Maxwell–Wagner space charge polarization, which is inherently a non-uniform charge accumulation.^[17] The measured capacitance per unit area of SAM- $\text{AlO}_y/\text{TiO}_x$ slightly varied on different devices because the spin-coating process was not able to yield the $\text{AlO}_y/\text{TiO}_x$ layer of uniform thickness. Summarized in Table 1 is the average capacitance per unit

Table 1: Capacitance per unit area (C_i), contact angle, and surface energy of the SAM-modified $\text{AlO}_y/\text{TiO}_x$ dielectrics.

SAM	C_i (nF/cm ²) ^[a] for SAM- $\text{AlO}_y/\text{TiO}_x$	Contact angle (°)		Surface energy (10 ⁻³ N/m)		
		water	CH_2I_2	γ^D	γ^P	$\gamma^{[b]}$
ODPA	200 ± 12	104.2	63.1	26.4	0.24	26.6
PA1	250 ± 18	75.2	42.8	37.6	5.4	43.0
PA2	240 ± 22	81.9	47.0	35.4	3.7	39.1
PA3	230 ± 23	88.1	49.2	34.2	2.1	36.3
PA4	280 ± 18	70.0	41.6	38.2	7.9	46.1
PA5	300 ± 23	64.4	29.7	43.7	8.9	52.6

[a] Measured at 100 Hz. [b] $\gamma = \gamma^D + \gamma^P$.

area of SAM- $\text{AlO}_y/\text{TiO}_x$ taken at the lowest frequency (100 Hz). It is found that the SAMs with more oxygen atoms in the chain and the oxygen atom closer to the surface lead to higher capacitance per unit area. From the same metal-insulator-metal structure, leakage current was measured. As shown in the Supporting Information, it is found that the SAMs of **PA1–5** generally reduce the leakage current from the $\text{AlO}_y/\text{TiO}_x$ dielectric, but not as effectively as the SAM of ODPA. A careful comparison indicates that the SAMs with more oxygen atoms in the chain and the oxygen atom closer to the surface lead to higher leakage currents.

To test whether **PA1–5** can lead to SAMs with enhanced surface energy, we measured the contact angles on the SAMs of **PA1–5** and ODPa using distilled water and diiodomethane (CH_2I_2) as the probe liquids,^[18] whose surface energies are known.^[19] We then calculated the dispersion and polar components of the surface energy for the SAM surfaces using Equation (1)

$$(1 + \cos \theta)\gamma_i = (\gamma_s^D \gamma_l^D)^{1/2} + 2(\gamma_s^P \gamma_l^P)^{1/2} \quad (1)$$

which is derived from the Owens-Wendt-Kaelble and Young's equations.^[20] Where θ is the equilibrium contact angle made by each liquid on the solid surface, γ is the surface energy. The superscripts *D* and *P* refer to the dispersive and the polar components, respectively, and the subscripts *l* and *s* refer to the liquid and solid, respectively.^[5] As summarized in Table 1, the oxygen-inserted phosphonic acids **PA1–5** generally have greater surface energy than ODPa by increasing both the polar and the dispersion components. The increased polar component can be attributed to the fact that oxygen is more electronegative than carbon and thus increases the dipole moment in **PA1–5**. The increased dispersion component is related to the lone pairs of electrons in oxygen, which lead to stronger interactions between induced dipoles. The surface energy of **PA1**, **PA4**, and **PA5** is higher than that of HMDS on SiO_2 ($40.5 \times 10^{-3} \text{ Nm}^{-1}$), and the surface energy of **PA5** is higher than that of PTS on SiO_2 ($48.3 \times 10^{-3} \text{ Nm}^{-1}$).^[21] More detailed findings from Table 1 regarding structure–property relationships are that the surface energy increases in the order of **PA3**, **PA2**, and **PA1** and in the order of **PA1**, **PA4**, and **PA5**. This indicates that the surface energy increases with the oxygen atom moving from the inside to the surface and with the number of oxygen atoms increasing.

With the enhanced surface energy, the $\text{AlO}_y/\text{TiO}_x$ dielectrics modified with **PA1–5** were found completely wettable by a variety of organic solvents, such as chloroform, isopropanol, ethyl acetate and toluene, with static contact angles smaller than 5° . Such good wettability brought considerable freedom to our experiments of optimizing solvents for drop casting. It was found that a mixed solvent of dichloromethane and acetone (1:1) yielded the best films of TIPS-TAP for OTFTs. In agreement with its relatively low surface energy, the SAM of **PA3** appeared less wettable by some organic solvents. For example, the measured contact angle of trichloroethene is 32° on **PA3**, but smaller than 5° on the other four oxygen-containing phosphonic acids.

As shown in Figure 2a, crystallization from a drop of solution of TIPS-TAP in dichloromethane and acetone (1:1) on the high-surface-energy SAMs (**PA1**, **PA2**, **PA4**, and **PA5**) led to continuous films containing highly ordered and well-connected crystalline fibers. During this crystallization, the contact diameter of the droplet on the surface remained almost constant with decreasing contact angle as the solvents evaporated. Such phenomenon is known as the pinned contact line, which is also observed during the crystallization of 6,13-bis((triisopropylsilyl)ethynyl)pentacene on high-surface-energy dielectrics as reported.^[22] In contrast, crystallization from a drop of the same solution on the SAMs with lower surface energy (**PA3** and ODPa) was found to

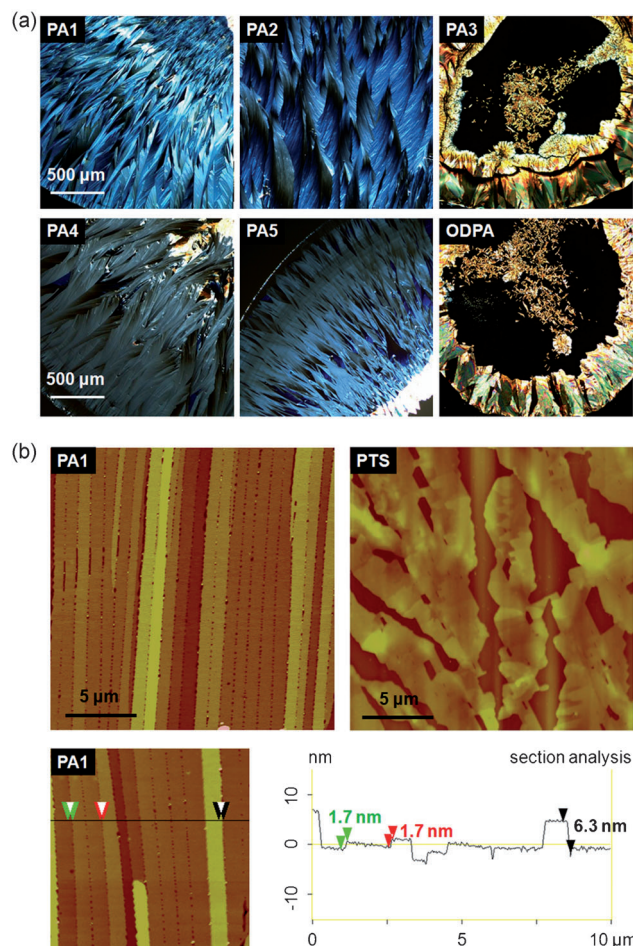


Figure 2. a) Reflected polarized-light micrographs for the films of TIPS-TAP that were cast from a solution in dichloromethane and acetone (1:1) onto the $\text{AlO}_y/\text{TiO}_x$ dielectric surface modified with various SAMs; b) AFM images for a drop-cast film of TIPS-TAP on **PA1**- and PTS-modified SiO_2 and section analysis for a drop-cast film of TIPS-TAP on **PA1**-modified $\text{AlO}_y/\text{TiO}_x$.

accompany shrinkage of the droplet and depinning of the contact line,^[23] leading to smaller films containing thick crystals^[24] at the periphery and isolated small crystals in the center. Neither of these crystals was suitable for fabricating OTFTs. The two types of crystallization observed indicate that the surface energy of the substrate is a key factor in governing the crystallization behavior of organic semiconductors from solutions.

The drop-cast films of TIPS-TAP on **PA1**, **PA2**, **PA4**, and **PA5** were then studied with X-ray diffraction (XRD) and atomic force microscopy (AFM). The X-ray diffraction patterns from the films have four diffraction peaks at $2\theta = 5.34^\circ$ (*d* spacing of 16.56 \AA), $2\theta = 10.68^\circ$ (*d* spacing of 8.28 \AA), $2\theta = 16.04^\circ$ (*d* spacing of 5.52 \AA), and $2\theta = 26.88^\circ$ (*d* spacing of 3.31 \AA). These diffractions agree with the (001), (002), (003), and (005) diffractions derived from the single-crystal structures indicating a highly ordered film with layered structures. A typical AFM image for these films is displayed in Figure 2b showing a smooth surface containing highly ordered flat micro-strips approximately $1 \mu\text{m}$ wide. Section

analysis reveals a molecular step of about 1.7 nm high, which is in agreement with the layer spacing of 16.56 Å. In contrast, the drop-cast films of TIPS-TAP on the PTS- and HMDS-modified SiO₂ surface exhibit very different morphologies having a much rougher surface with less ordered dendritic domains as shown in Figure 2b. However, it remains unclear how the two types of film morphologies are related to the terminal group and ordering of SAMs.

OTFTs were fabricated by depositing a layer of gold through a shadow mask onto the drop-cast films of TIPS-TAP to form top-contact source and drain electrodes. The resulting devices had highly doped silicon as the gate electrode and the SAM-modified AlO_y/TiO_x as dielectrics. The field effect mobility of these OTFTs in the saturation regime were measured under vacuum and extracted from transfer *I*-*V* curves at a drain voltage of 3 V using the equation: $I_{DS} = (\mu WC_i/2L)(V_G - V_T)^2$, where I_{DS} is the drain current, μ is field effect mobility, C_i is the capacitance per unit area for the SAM-modified AlO_y/TiO_x as listed in Table 1, W is the channel width, L is the channel length, and V_G and V_T are the gate and threshold voltage, respectively. It is found that the measured field effect mobility varied in different areas of the drop-cast thin films because these films are not homogeneous on the millimeter scale but contain a central region of smaller crystals and a peripheral region of larger crystals as shown in the polarized-light micrograph in Figure 3a. Summarized in Table 2 are the field effect mobilities as measured from the two types of areas in the OTFTs of TIPS-TAP, which were fabricated on different

Table 2: Measured field effect mobilities of TIPS-TAP films as drop-cast on different SAMs.^[a]

SAMs	Field effect mobility (cm ² /Vs)				Average of all channels
	Channels on large crystals range	Channels on large crystals average	Channels on small crystals range	Channels on small crystals average	
PA1	1.1–2.5	1.6	0.25–0.79	0.57	1.2
PA2	1.0–1.4	1.1	0.32–0.81	0.59	0.88
PA4	1.0–1.8	1.3	0.26–0.90	0.50	0.94
PA5	1.0–1.8	1.2	0.22–0.93	0.61	0.97

[a] Films drop-cast on PA3 were not suitable for fabrication of OTFTs.

SAM-modified dielectrics. It is found that the large crystals of TIPS-TAP in the drop-cast films on the SAMs of **PA1**, **PA2**, **PA4** and **PA5** generally exhibit electron mobility above 1 cm² V⁻¹ s⁻¹. In comparison, the channels on small crystals exhibit average electron mobility of around 0.5 to 0.6 cm² V⁻¹ s⁻¹. These mobilities are at least two orders of magnitude higher than that of TIPS-TAP films cast on PTS and HMDS, and can be attributed to the highly ordered and well-connected flat micro-stripes shown in Figure 2b. On the other hand, the low field effect mobility of TIPS-TAP films on the PTS and HMDS-modified SiO₂ may be attributed to the poor film morphology shown in Figure 2b. Shown in Figure 3b are the transfer *I*-*V* curves for the best-performing OTFT of TIPS-TAP fabricated on **PA1**-modified AlO_y/TiO_x dielectric, which exhibits a field-effect mobility of 2.5 cm² V⁻¹ s⁻¹ and an on/off ratio of 6 × 10⁵ for drain current between 0.6 and 3 V gate bias. The relatively high current of approximately 1 nA at 0 V gate bias is similar to that of the vacuum-deposited OTFTs on the bare AlO_y/TiO_x dielectrics as reported earlier^[14] and can be attributed to the gate leakage current arising from the spin-coated AlO_y/TiO_x dielectric.

Inserting oxygen atoms into the alkyl chains of SAM molecules can also, in principle, affect the performance of OTFTs in terms of threshold voltage and device stability in air because the polar oxygen atoms may produce a built-in electric field by increasing the molecular dipole moment^[25] and help to accumulate water molecules at the semiconductor–dielectric interface by hydrogen bonding. To check these effects, OTFTs of TIPS-TAP were fabricated by vacuum deposition onto the ODPa-modified AlO_y/TiO_x dielectric and used as a reference because drop-casting a solution of TIPS-TAP onto such a low-surface-energy surface only led to thick crystals unsuitable for OTFTs or thin films with low field effect mobility. It is found that the vacuum-deposited OTFTs with ODPa-modified dielectric exhibited electron mobility in the range of 1.3 to 1.8 cm² V⁻¹ s⁻¹ and an average threshold voltage of 0.83 V when tested under vacuum. When the AlO_y/TiO_x were modified with **PA1**, **PA2**, **PA4**, and **PA5**, the average threshold voltage shifted to 0.9–1.2 V as detailed in the Supporting Information. Such a positively shifted threshold voltage can be attributed to the negatively charged oxygen atoms, which induce positive charges in the semiconductor layer at the interface. However, no correlation between the threshold voltage and the number and position of oxygen atoms could be determined because of the significant device-to-device variation. Moreover, the drop-cast OTFTs

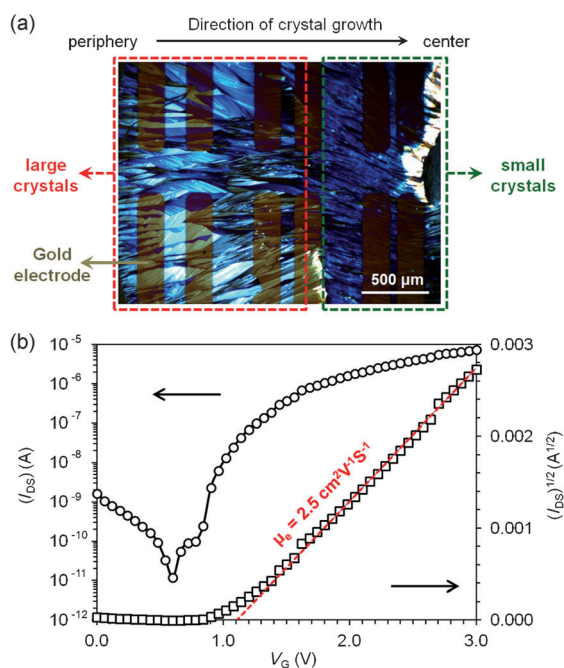


Figure 3. a) Reflected polarized-light micrograph for OTFTs of TIPS-TAP as cast from a solution in dichloromethane and acetone (1:1) onto the **PA1**-modified AlO_y/TiO_x. b) Drain current (I_{DS}) versus gate voltage (V_G) with drain voltage (V_{DS}) at 3 V for the best performing drop-cast OTFT of TIPS-TAP on the SAM of **PA1** with the active channel of $W=1$ mm and $L=150$ μm as measured under vacuum.

on the **PA1**-modified $\text{AlO}_y/\text{TiO}_x$ exhibited apparent hysteresis in their output and transfer I - V curves while the devices on ODPA-modified dielectric exhibited negligible hysteresis as shown in the Supporting Information. When a representative vacuum-deposited OTFT of TIPS-TAP on the ODPA-modified $\text{AlO}_y/\text{TiO}_x$ dielectric was tested in ambient air, the measured mobility decreased to about $0.35 \text{ cm}^2 \text{ V}^{-1} \text{ s}^{-1}$. In comparison, a representative drop-cast OTFT of TIPS-TAP on **PA1**-modified dielectric exhibited even lower mobility of about $0.02 \text{ cm}^2 \text{ V}^{-1} \text{ s}^{-1}$ in ambient air. This lower air stability as well as greater hysteresis associated with oxygen-inserted SAMs can be attributed to easier adhesion of water molecules to the high-surface-energy dielectric, which lead to more traps for electrons.

To test whether the SAMs of these oxygen-inserted phosphonic acids can be used as a general platform for solution-processed OTFTs, 6,13-bis((triisopropylsilyl)ethynyl)pentacene (TIPS-PEN), an established solution-processable p-type semiconductor, was also drop-cast onto **PA1**- and **PA4**-modified $\text{AlO}_y/\text{TiO}_x$ as detailed in the Supporting Information. It is found that the resulting p-channel transistors exhibited average field effect mobilities of 1.1 and $0.95 \text{ cm}^2 \text{ V}^{-1} \text{ s}^{-1}$, respectively, which are larger than the reported average mobility ($0.65 \text{ cm}^2 \text{ V}^{-1} \text{ s}^{-1}$) for solution-processed OTFTs of TIPS-PEN on HMDS-modified dielectrics of SiO_2 .^[26]

In conclusion, this work demonstrates a new strategy of interface engineering for high-performance solution-processed OTFTs by designing and synthesizing novel SAMs. The key of this strategy is to enhance the surface energy of SAMs by inserting polar oxygen atoms into the long alkyl chain of phosphonic acids. The SAMs of these new phosphonic acids on a solution-processed high- k $\text{AlO}_y/\text{TiO}_x$ layer, except that of **PA3**, have led to solution-processed n-channel OTFTs of TIPS-TAP with high field effect mobilities of up to $2.5 \text{ cm}^2 \text{ V}^{-1} \text{ s}^{-1}$ as well as low operation voltages. In association with its relatively low surface energy, the SAM of **PA3** has led to unfavorable crystallization of organic semiconductors. This result suggests that in this design the oxygen atom should be located at most two carbon atoms away from the SAM surface to reach a sufficient surface energy suitable for solution-based processing. As suggested by our preliminary results on solution-processed p-channel OTFTs of TIPS-PEN on **PA1**- and **PA4**-modified $\text{AlO}_y/\text{TiO}_x$, these novel high-surface-energy SAMs can be used as a general platform for high-performance solution-processed OTFTs.

Received: January 15, 2013
Published online: May 3, 2013

Keywords: organic thin-film transistors · phosphonic acids · self-assembly · semiconductors · surface chemistry

- [1] S. Onclin, B. J. Ravoo, D. N. Reinhoudt, *Angew. Chem.* **2005**, *117*, 6438–6462; *Angew. Chem. Int. Ed.* **2005**, *44*, 6282–6304.
- [2] a) J. Jang, *Mater. Today* **2006**, *9*, 46–52; b) G. Gelinck, P. Heremans, K. Nomoto, T. Anthopoulos, *Adv. Mater.* **2010**, *22*, 3778–3798.

- [3] a) T. Someya, A. Dodabalapur, J. Huang, K. C. See, H. E. Katz, *Adv. Mater.* **2010**, *22*, 3799–3811; b) J. T. Mabeck, G. G. Malliaras, *Anal. Bioanal. Chem.* **2006**, *384*, 343–353.
- [4] For examples on SAMs of phosphonic acids for interface engineering of OTFTs, see: a) H. Ma, O. Acton, D. O. Hutchins, N. Cernetic, A. K.-Y. Jen, *Phys. Chem. Chem. Phys.* **2012**, *14*, 14110–14126; b) K.-C. Liao, A. G. Ismail, L. Kreplak, J. Schwartz, I. G. Hill, *Adv. Mater.* **2010**, *22*, 3081–3085.
- [5] P. H. Wöbkenberg, J. Ball, F. B. Kooistra, J. C. Hummelen, D. M. de Leeuw, D. D. C. Bradley, T. D. Anthopoulos, *Appl. Phys. Lett.* **2008**, *93*, 013303.
- [6] For examples of surface-selective deposition by controlling the wettability of the dielectric surface with patterned SAMs, see: a) S. K. Park, D. A. Mourey, S. Subramanian, J. E. Anthony, T. N. Jackson, *Adv. Mater.* **2008**, *20*, 4145–4147; b) H. S. Lee, D. Kwak, W. H. Lee, J. H. Cho, K. Cho, *J. Phys. Chem.* **2010**, *114*, 2329–2333; c) T. Minari, C. Liu, M. Kano, K. Tsukagoshi, *Adv. Mater.* **2012**, *24*, 299–306; d) T. Minari, M. Kano, T. Miyadera, S.-D. Wang, Y. Aoyagi, M. Seto, T. Nemoto, S. Isoda, K. Tsukagoshi, *Appl. Phys. Lett.* **2008**, *92*, 173301.
- [7] Y. Chung, E. Verploegen, A. Vailionis, Y. Sun, Y. Nishi, B. Murmann, Z. Bao, *Nano Lett.* **2011**, *11*, 1161–1165.
- [8] Y. Ito, A. A. Virkar, S. Mannsfeld, J. H. Oh, M. Toney, A. Locklin, Z. Bao, *J. Am. Chem. Soc.* **2009**, *131*, 9396–9404.
- [9] J. M. Ball, P. H. Wöbkenberg, F. Colléaux, M. Heeney, J. E. Anthony, I. McCulloch, D. D. C. Bradley, T. D. Anthopoulos, *Appl. Phys. Lett.* **2009**, *95*, 103310.
- [10] S. Miao, A. L. Appleton, N. Berger, S. Barlow, S. R. Marder, K. I. Hardcastle, U. H. F. Bunz, *Chem. Eur. J.* **2009**, *15*, 4990–4993.
- [11] Z. Liang, Q. Tang, J. Xu, Q. Miao, *Adv. Mater.* **2011**, *23*, 1535–1539.
- [12] As found from the AFM section analysis, these bulk crystals were more than $1 \mu\text{m}$ thick and had a very rough surface. Direct deposition of source and drain electrodes of gold onto these thick crystals led to poor field effect transistors with electron mobility in the range of $10^{-5} \text{ cm}^2 \text{ V}^{-1} \text{ s}^{-1}$.
- [13] L. L. Chua, J. Zaumseil, J.-F. Chang, E. C.-W. Ou, P. K. H. Ho, H. Sirringhaus, R. Friend, *Nature* **2005**, *434*, 194–199.
- [14] Y. Su, C. Wang, W. Xie, F. Xie, J. Chen, N. Zhao, J. Xu, *ACS Appl. Mater. Interfaces* **2011**, *3*, 4662–4667.
- [15] O. Acton, D. Hutchins, L. Árnadóttir, T. Weidner, N. Cernetic, G. G. Ting, T.-W. Kim, D. G. Castner, H. Ma, A. K.-Y. Jen, *Adv. Mater.* **2011**, *23*, 1899–1902.
- [16] In the measurement of capacitance, thermal evaporated gold ($0.2 \text{ mm} \times 1 \text{ mm}$) was used as the top electrode and the highly doped silicon substrate was used as the bottom electrode. For examples of measuring the capacitance of phosphonic acid modified metal oxide dielectrics by the same method, see: a) O. Acton, G. Ting, H. Ma, J. W. Ka, H.-L. Yip, N. M. Tucker, A. K.-Y. Jen, *Adv. Mater.* **2008**, *20*, 3697–3701; b) O. Acton, G. Ting, H. Ma, A. K.-Y. Jen, *Appl. Phys. Lett.* **2008**, *93*, 083302.
- [17] a) S. Blonkowski, M. Regache, A. Halimaoui, *J. Appl. Phys.* **2001**, *90*, 1501–1508; b) S. Ramanathan, C. M. Park, P. C. McIntyre, *J. Appl. Phys.* **2002**, *91*, 4521–4527.
- [18] K.-J. Chang, F. Y. Yang, C. C. Liu, M. Y. Hsu, T. C. Liao, H. C. Cheng, *Org. Electron.* **2009**, *10*, 815–821.
- [19] The dispersion and polar components of the surface tension are 21.8 mN m^{-1} and 50.9 mN m^{-1} , respectively, for water, and 50.0 mN m^{-1} and 0 mN m^{-1} , respectively, for CH_2I_2 . See: Ref. [20].
- [20] D. Y. Kwok, A. W. Neumann, *Adv. Colloid Interface Sci.* **1999**, *81*, 167–249.
- [21] The surface energy for the SAMs of HMDS and PTS was measured using the same method as described above.
- [22] J. H. Lim, W. H. Lee, D. Kwak, K. Cho, *Langmuir* **2009**, *25*, 5404–5410.

- [23] Similar shrinkage of solution droplets and depinning of contact line were also observed during the crystallization of 6,13-bis(triisopropylsilyl)ethynyl-pentacene on low-surface-energy dielectrics as reported in Ref. [22].
- [24] As found from the AFM section analysis, these bulk crystals are more than 1 μm thick and have very rough surfaces.
- [25] S. Kobayashi, T. Nishikawa, T. Takenobu, S. Mori, T. Shimoda, T. Mitani, H. Shimotani, N. Yoshimoto, S. Ogawa, Y. Iwasa, *Nat. Mater.* **2004**, 3, 317–322.
- [26] S. K. Park, T. N. Jackson, J. E. Anthony, D. A. Mourey, *Appl. Phys. Lett.* **2007**, 91, 063514.
-